Acta Oceanol. Sin., 2020, Vol. 39, No. 7, P. 165–174
https://doi.org/10.1007/s13131-020-1624-y
http://www.hyxb.org.cn
E-mail: hyxbe@263.net

Two-step harmonic analysis for capturing seasonally-varying amplitudes and phase lags of the predominant tidal constituents

Anzhou Cao[1], Zheng Guo[2]*

[1] Ocean College, Zhejiang University, Zhoushan 316021, China

[2] Marine Science and Technology College, Zhejiang Ocean University, Zhoushan 316021, China

Received 5 October 2019; accepted 19 November 2019

Abstract

Recent studies have revealed that the predominant tidal constituents have seasonal variations at some locations. However, how to accurately obtain these variations remains a problem for the traditional harmonic analysis (HA) due to the tradeoff between length of time window and resolution of constituents. Therefore, a method named as "two-step HA" is developed in this study, which consists of both long- and short-time-window HA. Through a series of ideal experiments, practical application at two tidal gauges and comparison with the traditional HA, the feasibility and accuracy of the two-step HA are verified: The two-step HA performs better than the traditional HA in estimating monthly amplitudes and phases for the predominant constituents, whether they have seasonal variability or not. In addition to capturing variations of the predominant constituents at tidal gauges, the two-step HA would be useful in investigation of the coherence and incoherence of internal tides.

Key words: tides, harmonic analysis, seasonal variation, tidal gauges

Citation: Cao Anzhou, Guo Zheng. 2020. Two-step harmonic analysis for capturing seasonally-varying amplitudes and phase lags of the predominant tidal constituents. Acta Oceanologica Sinica, 39(7): 165–174, doi: 10.1007/s13131-020-1624-y

1 Introduction

Tides are one ubiquitous motion in oceans. They are caused by a combination of time-varying gravitational potential of the moon and sun and the centrifugal forces generated as earth rotates about the common center of mass of the earth-moon-sun system (Stewart, 2008). The investigation of tides has a long history. Kelvin, Ferrel, Darwin, Doodson (1921, 1924, 1928) and other great scholars developed and refined the harmonic analysis (HA) method for tidal analysis and prediction (Goldsbrough, 1942; Foreman and Henry, 1989). Up to now, HA has been realized with Fortran and Matlab codes (Godin, 1972; Foreman, 1977; Pawlowicz et al., 2002; Codiga, 2011) and widely used in the analysis of tides and other ocean dynamics related to tides. According to the traditional HA, the surface elevation induced by each constituent is expressed as

$$\xi_n(t) = f_n h_n \cos(\omega_n t + u_n - g_n), \quad (1)$$

where subscript n denotes different tidal constituents, t is the time, ω is the angular frequency, h and g are the amplitude and phase lag (the well-known harmonic constants), f and u are the nodal factor and angle which vary slowly with a period of 18.61 years. In the conventional wisdom, amplitude and phase lag of each constituent at a certain location would not vary with time.

With the accumulation of water elevation data from global tidal gauges and altimetry satellites, some observations are found to deviate from the conventional wisdom, i.e., the observed tidal amplitudes and phase lags are found to have seasonal variations (Huess and Andersen, 2001; Kang et al., 2002; St-Laurent et al., 2008; Georgas, 2012; Gräwe et al., 2014; Müller et al., 2014), secular changes (Ray, 2006, 2009; Jay, 2009; Müller et al., 2011) and nodal cycles differing from theoretical predictions (Amin, 1985; Ray, 2006; Cherniawsky et al., 2009; Feng et al., 2015). By reviewing previous studies, Woodworth (2010) summarized that a combination of five dynamical and three technical causes could partly account for the long-term changes in tidal amplitudes and phase lags. However, as also indicated by Woodworth (2010), the reasons for seasonal variability in tidal amplitudes and phase lags remain far to be fully understood.

How to accurately obtain seasonally-varying amplitudes and phase lags of the predominant constituents is also a problem for the traditional HA. Because a tradeoff between length of time window and resolution of constituents always exists in the traditional HA, using a long time window yields long-time-averaged amplitudes and phase lags which would differ from the real values of varying amplitudes and phase lags; while a short time window cannot resolve sufficient constituents, so that the unresolved constituents influence the amplitudes and phase lags of the resolved constituents. Therefore, a new way to implement HA is developed in this study. It combines long- and short-time-window HA. To distinguish from the traditional HA, it is named as "two-step HA" for convenience. The feasibility and accuracy of the two-step HA is validated by a series of ideal experiments (IEs) and compared with traditional HA using one-month (St-Laurent et al., 2008; Müller et al., 2014) and three-month (Huess and Andersen, 2001) windows.

The paper is organized as follows. The two-step HA is introduced in Section 2. Performances of the two-step HA in a series of IEs are shown in Section 3. In Section 4, the two-step HA is applied to practical scenario to investigate the seasonal variability

Foundation item: The National Natural Science Foundation of China under contract No. 41806012.
*Corresponding author, E-mail: guozheng-gz@163.com

of the predominant constituents at two tidal gauges. Finally, a discussion and a summary complete the paper in Section 5.

2 Methodology

Generally, the K_1, O_1, M_2 and S_2 constituents are recognized as the predominant diurnal and semidiurnal constituents in oceans. To accurately capture their seasonally-varying amplitudes and phase lags is the main aim of this study. According to Fang et al. (2004), the Rayleigh criterion for each pair of eight constituents corresponding to hourly measurements is calculated and shown in Table 1. As shown, a record longer than 15 d with hourly intervals is sufficient to separate the K_1, O_1, M_2 and S_2 constituents from most of the other constituents; but it cannot resolve the constituent pair of P_1 and K_1 as well as that of the K_2 and S_2, which leads to incorrect estimations for the K_1 and S_2 (Amin, 1985). Therefore, to obtain accurate estimations for the K_1 and S_2 constituents, we need to firstly extract the P_1 and K_2 from a relatively long record (e.g., a one-year record) according to Table 1. This is the core of the two-step HA and detailed procedure is introduced as follows.

Table 1. Alias periods (d) for each pair of constituents corresponding to hourly measurements based on the Rayleigh criterion

	O_1	P_1	**K_1**	N_2	M_2	S_2	**K_2**
Q_1	27.6	9.6	9.1	1.0	1.0	0.9	0.9
O_1		14.8	13.7	1.0	1.0	0.9	0.9
P_1			**182.6**	1.1	1.1	1.0	1.0
K_1				1.1	1.1	1.0	1.0
N_2					27.6	9.6	9.1
M_2						14.8	13.7
S_2							**182.6**

Note: The unresolved constituent pairs (K_1 and P_1 as well as K_2 and S_2) by a one-month record and their alias periods are marked in bold.

Step one: The whole observation record is divided into several one-year segments and the traditional HA is performed for each one-year segment ξ with the U_Tide Matlab package (Codiga, 2011). For a one-year (common year of 365 d) record, U_Tide would automatically choose 59 constituents. Thereafter, a one-year hindcast η is calculated using 55 of the 59 constituents except the K_1, O_1, M_2 and S_2. Subtracting η from ξ, a one-year record ζ only related to the K_1, O_1, M_2 and S_2 constituents is obtained.

Step two: The one-year record ζ is divided into twelve uniform 30-day segments corresponding to twelve months. For each month except February, the segment lasts from 1 to 30, while the segment of February starts on 31 January and ends on 1 March (29 February) for common (leap) years. Thereafter, the traditional HA is performed for each 30-day segment to obtain the monthly amplitudes and phase lags of the K_1, O_1, M_2 and S_2 constituents.

Note that for the 366-day record of a leap year, U_Tide would automatically choose 67 constituents. Compared with the 365-day record of a common year, 8 more constituents, the S_a, π_1, S_1, ψ_1, H_1, H_2, T_2 and R_2, are automatically resolved. To be consistent with common years, only the record of the first 365 d in leap years is used for analysis. In addition, the T_Tide Matlab package (Pawlowicz et al., 2002) can serve as an alternative to U_Tide in the two-step HA.

3 Validation by IEs

In this section, a series of IEs are designed to validate the feasibility and accuracy of the two-step HA. In these IEs, a 365-day-time series is synthesized:

$$\zeta(t) = S_0 + \sum_{n=1}^{8} h_n \cos(\omega_n t - g_n) + \varepsilon(t), \tag{2}$$

where S_0=20 cm is the mean water level, ε denotes the measurement error with a maximum value of 5 cm, and n=1,2,...,8 represents the Q_1, O_1, P_1, K_1, N_2, M_2, S_2, K_2 constituents, respectively. Note that the nodal correction and angle are neglected in this study, as they can be obtained through a fitting of the calculated amplitudes and phase lags (Ray, 2006; Feng et al., 2015).

In IE1, all the eight constituents are assumed to have constant amplitudes and phase lags, of which the prescribed values are shown in Table 2. Note that the ratios of prescribed amplitudes among both diurnal and semidiurnal constituents are consistent with those for the equilibrium tide.

Table 2. Prescribed amplitudes (cm) and phase lags (°) of the eight constituents in IE 1

	Q_1	O_1	P_1	K_1	N_2	M_2	S_2	K_2
h	14	71	33	100	19	100	47	13
g	310	90	270	250	20	280	100	140

Figure 1 displays the monthly amplitudes and phase lags of the four predominant constituents calculated with the traditional HA using a 30-day window. Note that the constituents are automatically determined by U_Tide, and only the amplitudes and phase lags of the O_1, K_1, M_2 and S_2 constituents are shown. The amplitudes and phase lags of the O_1 and M_2 constituents are close to the prescribed values, but there still exist small deviations. The mean absolute errors (MAEs) between the O_1 and M_2 amplitudes and their prescribed values are 1.6 and 0.4 cm, respectively. Note that these deviations are not caused by the measurement error ε, because these deviations still exist even if we remove the measurement error from the one-year time series (Eq.(2)). In other words, these deviations are related to the choice of the 30-day window. When a longer time window (e.g. one year) is used, these deviations decrease significantly and even vanish if the measurement error is not taken into consideration. For the K_1 and S_2 constituents, unrealistic semiannual cycles are found in their amplitudes and phase lags, which are caused by the unresolved P_1 and K_2 constituents explained above. If the monthly K_1(S_2) amplitudes (Figs 1b and d) are fitted using the following function:

$$A(t) = A_0 + A_s \cos\left(\frac{2\pi}{T_s}t - \phi\right), \tag{3}$$

where T_s equals to half of a year, the calculated A_0 and A_s are close to the prescribed K_1 (S_2) and P_1 (K_2) amplitudes, respectively. The MAEs between the K_1 and S_2 amplitudes and their prescribed values are 20.6 and 8.2 cm, respectively. In addition, the traditional HA using a three-month window leads to a similar result with slightly smaller MAEs, which are not shown.

In contrast to the traditional HA, the two-step HA provides a more accurate estimation. As shown in Fig. 2, the monthly amplitudes and phase lags of the four predominant constituents are almost the same as the prescribed values. The unrealistic semi-

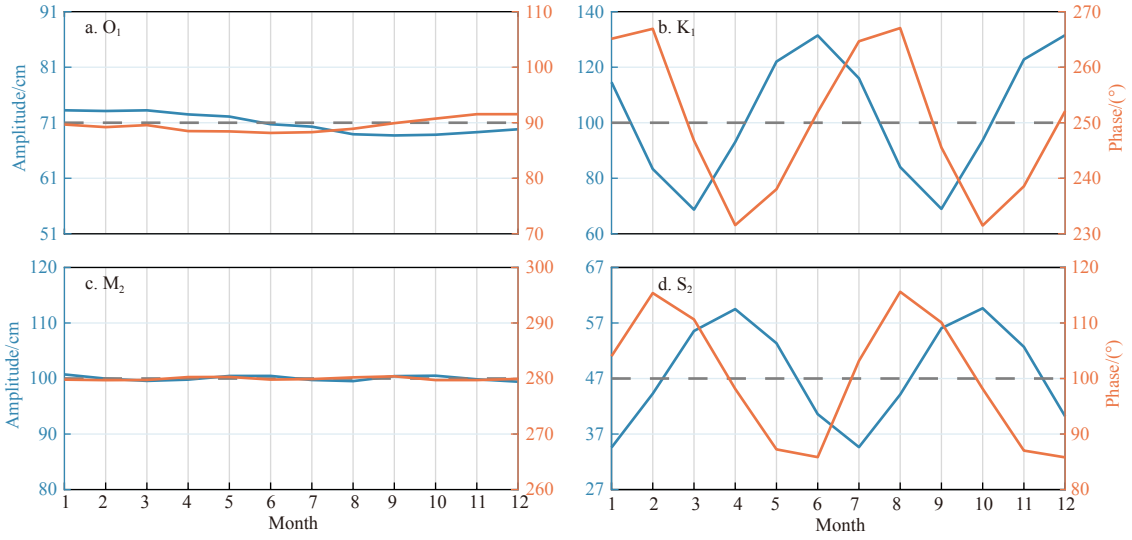

Fig. 1. Monthly amplitudes (blue solid lines) and phase lags (orange solid lines) of the O_1 (a), K_1 (b), M_2 (c) and S_2 (d) constituents for traditional HA using a one-month window in IE 1. The dashed line in each subfigure denotes the prescribed values of amplitudes and phase lags.

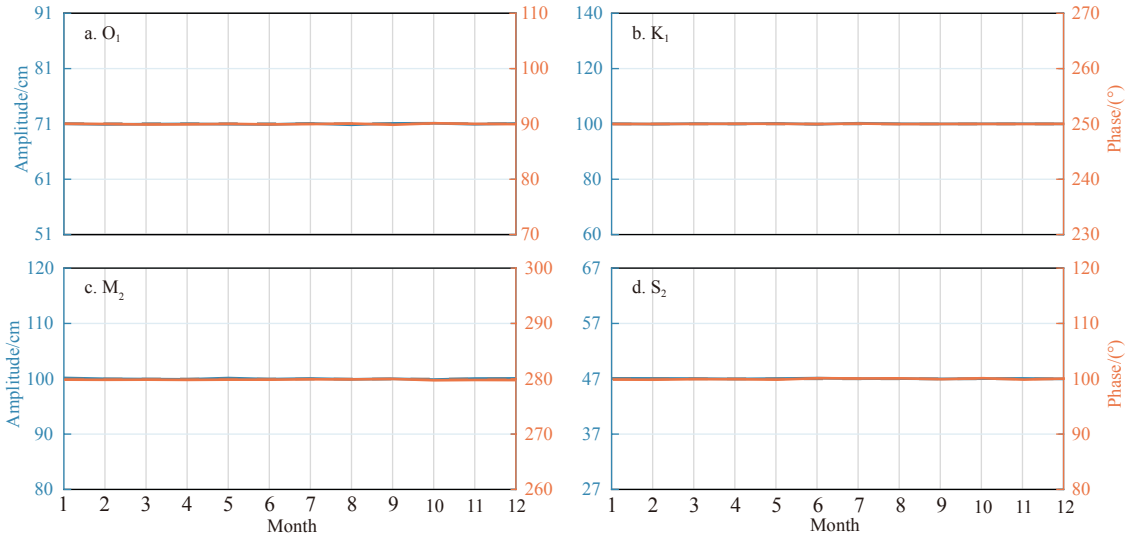

Fig. 2. Monthly amplitudes (blue solid lines) and phase lags (orange solid lines) of the O_1 (a), K_1 (b), M_2 (c) and S_2 (d) constituents for the two-step HA in IE 1. Both the prescribed and estimated amplitudes and phase lags are overlapped.

annual cycles (Figs 1b and d) are absent from the amplitudes and phase lags of the K_1 and S_2 constituents, suggesting that the two-step HA can indeed resolve the K_1 and S_2 constituents from the P_1 and K_2, respectively. The MAEs between the O_1, K_1, M_2 and S_2 amplitudes and their prescribed values are all less than 0.1 cm, which are at least one order of magnitude smaller than those using the traditional HA. Combining these results, it can be concluded that the two-step HA can provide an accurate estimation for the amplitudes and phase lags of the predominant constituents and perform better than the traditional HA using one- or three-month windows.

As the two-step HA can resolve the K_1 and S_2 constituents from the P_1 and K_2, its performances on estimating seasonally-varying amplitudes and phase lags are examined in the following IEs. In IE2, the $K_1$and S_2 constituents are assumed to have seasonal variability whereas the amplitudes and phase lags of the other six constituents are constant as listed in Table 2. The amplitudes and phase lags of the K_1 and S_2 constituents in IE2 are prescribed as

$$h_4(t) = 100 + 10\cos\left(\frac{2\pi}{T_a}t\right) \quad (\mathrm{cm}), \tag{4}$$

$$g_4(t) = 250 + 10\cos\left(\frac{2\pi}{T_a}t + \frac{\pi}{2}\right) \quad (^\circ), \tag{5}$$

$$h_7(t) = 47 + 4.7\cos\left(\frac{2\pi}{T_a}t - \frac{\pi}{2}\right) \quad (\mathrm{cm}), \tag{6}$$

$$g_7(t) = 100 + 10\cos\left(\frac{2\pi}{T_a}t\right) \quad (^\circ), \tag{7}$$

where T_a equals to 365 d. In IE3, the P_1 and K_2 constituents are assumed to have seasonal variability whereas the other six constituents remain invariant (Table 2). The amplitudes and phase lags of the P_1 and K_2 constituents in IE3 are prescribed as

$$h_3(t) = 33 + 3.3\cos\left(\frac{2\pi}{T_a}t\right) \quad (\mathrm{cm}), \tag{8}$$

$$g_3(t) = 270 + 10\cos\left(\frac{2\pi}{T_a}t + \frac{\pi}{2}\right) \quad (^\circ), \tag{9}$$

$$h_8(t) = 13 + 1.3\cos\left(\frac{2\pi}{T_a}t - \frac{\pi}{2}\right) \quad (\mathrm{cm}), \tag{10}$$

$$g_8(t) = 140 + 10\cos\left(\frac{2\pi}{T_a}t\right) \quad (^\circ). \tag{11}$$

In IE4, the P_1, K_1, S_2, K_2 constituents are assumed to be seasonally-varying and their amplitudes and phase lags are prescribed as Eqs (4–11) while the Q_1, O_1, N_2 and M_2 constituents remain invariant (Table 2). In IE 5, all the amplitudes and phase lags of the eight constituents are seasonally-varying. Amplitudes and phase lags of the P_1, K_1, S_2, K_2 constituents in IE 5 are the same as those in IE 4, and those of the Q_1, O_1, N_2 and M_2 are prescribed as follows:

$$h_1(t) = 14 + 1.4\cos\left(\frac{2\pi}{T_a}t\right) \quad (\mathrm{cm}), \tag{12}$$

$$g_1(t) = 310 + 10\cos\left(\frac{2\pi}{T_a}t + \frac{\pi}{2}\right) \quad (^\circ), \tag{13}$$

$$h_2(t) = 71 + 7.1\cos\left(\frac{2\pi}{T_a}t\right) \quad (\mathrm{cm}), \tag{14}$$

$$g_2(t) = 90 + 10\cos\left(\frac{2\pi}{T_a}t + \frac{\pi}{2}\right) \quad (^\circ), \tag{15}$$

$$h_5(t) = 19 + 1.9\cos\left(\frac{2\pi}{T_a}t - \frac{\pi}{2}\right) \quad (\mathrm{cm}), \tag{16}$$

$$g_5(t) = 20 + 10\cos\left(\frac{2\pi}{T_a}t\right) \quad (^\circ), \tag{17}$$

$$h_6(t) = 100 + 10\cos\left(\frac{2\pi}{T_a}t - \frac{\pi}{2}\right) \quad (\mathrm{cm}), \tag{18}$$

$$g_6(t) = 280 + 10\cos\left(\frac{2\pi}{T_a}t\right) \quad (^\circ). \tag{19}$$

Figures A1, A2 (in the Appendix) and 3 show the amplitudes and phase lags of the four predominant constituents estimated by the two-step HA in IEs 2–4, respectively. In IE 2, both the seasonally-varying amplitudes and phase lags of the K_1 and S_2 and constant amplitudes and phase lags of the O_1 and M_2 are successfully captured by the two-step HA (Fig. A1). The MAEs between the O_1, K_1, M_2 and S_2 amplitudes and their prescribed values are 0.2, 0.4, 0.2 and 0.3 cm, respectively. Although these MAEs are a little larger than those in IE1 using the two-step HA (less than 0.1 cm), they are still smaller than the MAEs for the traditional HA using a 30-day window (0.4–1.6 cm). These results indicate that if the P_1 and K_2 constituents are invariant, the seasonally-varying amplitudes and phases of the K_1 and S_2 can be accurately obtained through the two-step HA. When the P_1 and K_2 constituents are varying (IEs 3 and 4), the varying tendencies of the K_1 and S_2 can still be captured by the two-step HA, but the deviations in the K_1 and S_2 amplitudes and phase lags are increased (Figs A2 and 3). The MAEs between the O_1, K_1, M_2 and S_2 amplitudes and their prescribed values are 0.1, 3.0, 0.1 and 1.1 cm in IE 3 and 0.1, 2.9, 0.2 and 1.1 cm in IE 4. In these two IEs, MAEs of the O_1 and M_2 constituents are comparable to those in IE 2, while MAEs of the K_1 and S_2 are approximate one order of magnitude larger than those in IE 2. This result indicates the difficulty in accurately es-

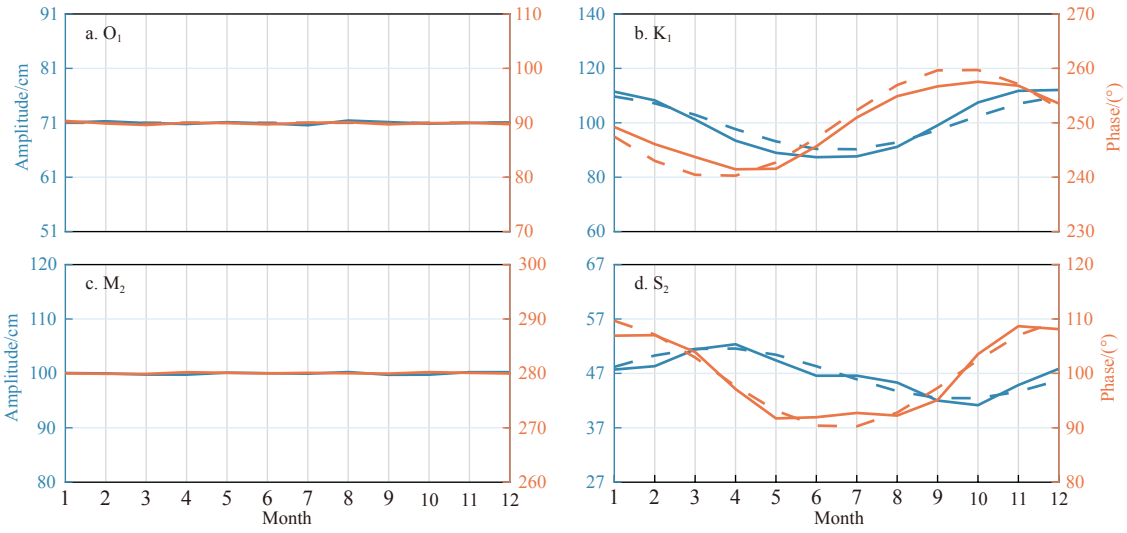

Fig. 3. Monthly amplitudes (blue solid lines) and phase lags (orange solid lines) of the O_1 (a), K_1 (b), M_2 (c) and S_2 (d) constituents for the two-step HA in IE 4. The dashed lines in b and d denote the prescribed amplitudes and phase lags at the center of each month.

timating the amplitudes and phase lags of the K_1 and S_2 with varying P_1 and K_2 constituents. To our knowledge, there is no other approach that can solve the problem with high accuracy. Combining the results shown in Figs A2 and 3 and the calculated MAEs, we believe that performances of the two-step HA in IEs 3 and 4 are acceptable, because (1) the amplitudes and phase lags estimated by the two-step HA generally capture the variation of the prescribed K_1 and S_2, and (2) MAEs of the K_1 and S_2 are smaller than their amplitudes as well as the maximum value of measurement error (5 cm).

Figure 4 illustrates the amplitudes and phase lags of the four predominant constituents estimated by the two-step HA in IE 5. Although all the eight prescribed constituents are seasonally-varying, the prescribed O_1 and M_2 constituents can be accurately obtained with MAEs of 0.4 and 0.7 cm in amplitudes; the MAEs between the K_1 and S_2 amplitudes and their prescribed values are 2.9 and 1.0 cm, which are comparable to those in IEs 3 and 4 and also acceptable. This result suggests that except the P_1 and K_2 constituents, variations of other constituents almost have no effects on the estimation of the K_1 and S_2, when using the two-step HA.

Combining all the results of IEs, it can be concluded that the two-step HA is a useful tool to estimate the seasonally-varying amplitudes and phase lags of the predominant constituents. Compared with the traditional HA using a short time (e.g., one-month) window, the two-step HA yields more accurate results and avoids the occurrence of unrealistic semiannual cycles caused by the unresolved constituents. In the next section, we will show the performance of the two-step HA dealing with real scenario.

4 Practical applications

Müller et al. (2014) have shown that the M_2 constituent exhibits apparent seasonality at Cuxhaven, Germany and Victoria, Canada. In this study, the two-step HA is applied to the water elevation records at the two tidal gauges. To be consistent with Müller et al. (2014), the records at Cuxhaven from 1986 to 2005 and those at Victoria from 1966 to 1985 are used, which are obtained from the University of Hawaii Sea Level Center (UHSLC, https://uhslc.soest.hawaii.edu/data/, Caldwell et al., 2015).

Figure 5 shows the monthly M_2 amplitudes at Cuxhaven using both the two-step and traditional HA. As a comparison, the monthly S_2 amplitudes are also displayed. On the whole, the monthly M_2 amplitudes using the two-step HA are generally consistent with those using the traditional HA. This is reasonable because the M_2 constituent is able to be resolved with a short record (Table 1). However, a little difference still exists between the monthly M_2 amplitudes using the two-step and traditional HA at some time. As a result, the 20-year-averaged monthly M_2 amplitudes obtained by the two-step HA have slightly smaller seasonal variation than those obtained by the traditional HA (Fig. 5c). At the same time, the 20-year-averaged monthly M_2 amplitudes obtained by the two-step HA have smaller standard deviations (STDs) than those obtained by the traditional HA (Fig. 5c). Combining this result and those in IEs, we believe that the two-step HA yields a more accurate estimation. In other words, the traditional HA using a 30-day window may slightly overestimate the seasonal variation in the M_2amplitude. In contrast to the M_2 constituent, the S_2 amplitudes obtained with the two-step HA are almost invariant throughout the year with small STDs (Fig. 5d). Whereas the traditional HA using a 30-day window yields unrealistic semiannual cycles with large STDs, which is accounted for by the unresolved K_2 constituent. Similar result is found for the K_1 and O_1 constituents at the tidal gauge (Fig. 6). The O_1 constituent obtained by the two-step and traditional HA is almost the same, whereas the traditional HA using a 30-day window yields unrealistic semiannual cycles for the K_1 constituent due to the unresolved P_1 constituent. Combining these results, it can be concluded that the two-step HA can yield a good estimation of the monthly amplitudes and phase lags for the predominant constituents, whether they exhibit seasonal variability or not. Similar results are found at the tidal gauge of Victoria, which are shown in Figs A3 and 4 in Appendix.

Müller et al. (2014) explored the dynamics behind the seasonal variation of the M_2 constituent based on an ocean circulation and tide model. They found that the seasonal change in stratification on the continental shelf and frictional effect between sea-ice and the surface ocean layer cause the seasonal variation of

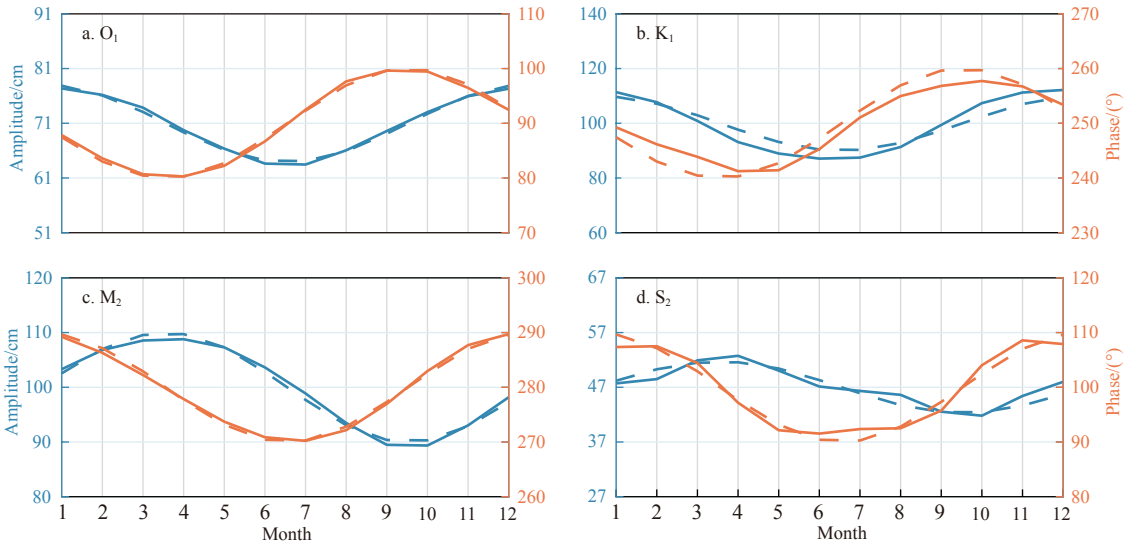

Fig. 4. Monthly amplitudes (blue solid lines) and phase lags (orange solid lines) of the O_1 (a), K_1 (b), M_2 (c) and S_2 (d) constituents for the two-step HA in IE 5. The dashed lines in each subfigure denote the prescribed amplitudes and phase lags at the center of each month.

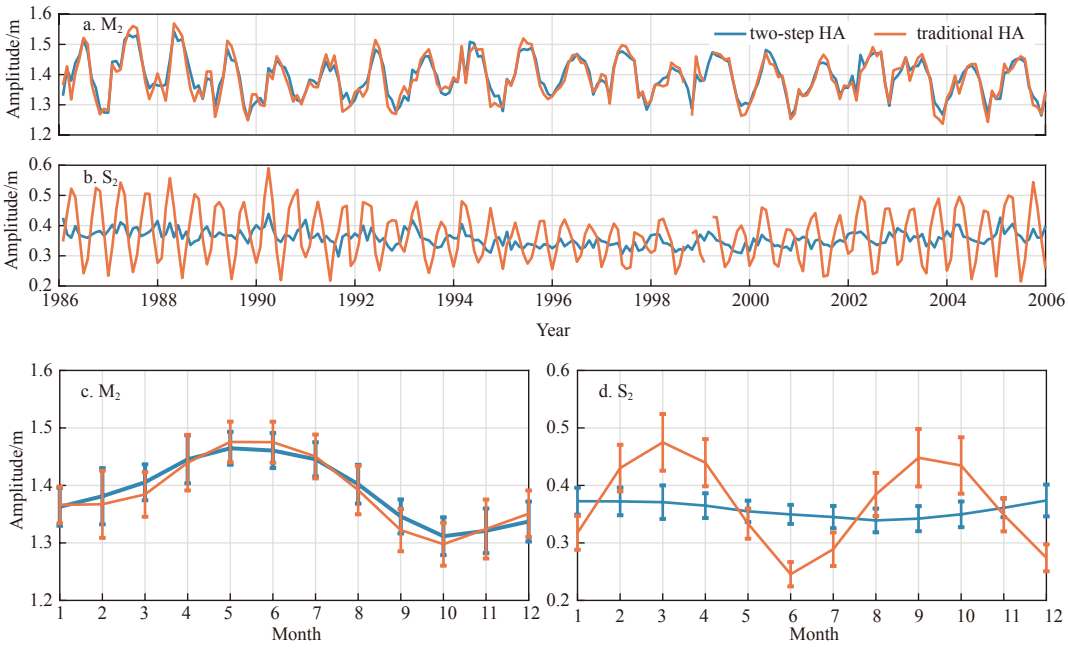

Fig. 5. Monthly amplitudes of the M_2 (a)and S_2 (b) constituents at Cuxhaven during 1986–2006, and the 20-year-averaged monthly amplitudes and corresponding STDs of the M_2 (c) and S_2 (d) constituents. In each subfigure, the blue and orange lines denote the results obtained by the two-step HA and traditional HA using a one-month window, respectively.

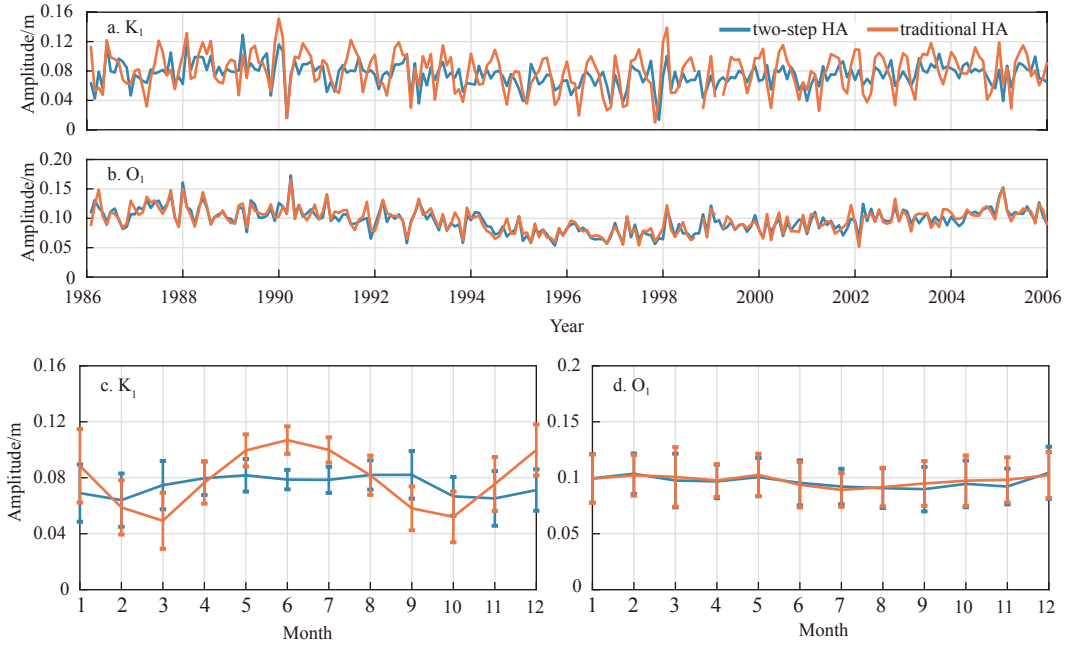

Fig. 6. Monthly amplitudes of the K_1 (a) and O_1 (b) constituents at Cuxhaven during 1986–2006, and the 20-year-averaged monthly amplitudes and corresponding STDs of the K_1 (c) and O_1 (d) constituents. In each subfigure, the blue and orange lines denote the results obtained by the two-step HA and traditional HA using a one-month window, respectively.

the M_2 constituent. However, results of this study show that there is no apparent seasonal variability for the S_2, K_1 and O_1 constituents. Why do these dynamical processes not influence the S_2, K_1 and O_1 constituents? It needs further exploration.

5 Discussion and summary

Recent studies have shown that amplitudes and phase lags of the predominant constituents exhibit seasonal variations at some locations (Huess and Andersen, 2001; Kang et al., 2002; St-Laurent et al., 2008; Georgas, 2012; Gräwe et al., 2014; Müller et al., 2014). However, how to accurately obtain these variations remains a problem for the traditional HA due to the tradeoff between the length of time window and resolution of constituents. A new way to implement HA, named as "two-step HA" to distinguish from the traditional HA, is developed to capture these variations, which consists of both long- and short-time-window

HA. Through a series of IEs, practical application to water elevation records at two tidal gauges as well as comparison with the traditional HA, the feasibility and accuracy of the two-step HA is verified: The two-step HA can provide a good estimation of monthly amplitudes and phase lags for the predominant constituents whether they have seasonal variability or not. The two-step HA also performs better than the traditional HA using one- or three-month windows: First, the two-step HA leads to smaller deviations than the traditional HA; Second, the traditional HA using one- or three-month windows causes unrealistic semiannual cycles in the amplitudes and phase lags of the K_1 and S_2 constituents due to the influence of the unresolved P_1 and K_2, whereas the two-step HA avoids it.

Several methods have been proposed to capture the variations of the predominant constituents. For instance, the tidal admittances, which are the complex ratios of the harmonic constants of the observed tide versus the equilibrium tide, have been used to investigate the tidal seasonality (Devlin et al., 2018). Based on the traditional HA, an interpolation method and an independent point (IP) scheme, Jin et al. (2018) and Guo et al. (2018) put forward two methods to capture variations of harmonic parameters. Jin et al. (2018) adopted the cubic spline interpolation while Guo et al. (2018) employed the linear interpolation. Each method has its own advantages. The two-step HA introduced in this study is easy to realize based on existing Matlab packages such as U_tide and T_tide. It calculates harmonic constants with temporal changes while avoids introducing unrealistic fluctuations.

The two-step HA introduced in this study is validated as a useful tool to capture varying amplitudes and phase lags of the predominant constituents. In the near future, we will apply it to water elevation records at global tidal gauges and provide a global map of seasonal variability for the predominant constituents, which we hope to be helpful to understanding the dynamics lying behind. In addition, we will also apply the two-step HA to current observations to investigate the variations of internal tides, because mesoscale eddies with lifecycles of months to years can scatter the internal tidal energy (Dunphy and Lamb, 2014) so as to change the current ellipses of internal tides over a period. This is meaningful and important when investigating the coherence and incoherence of internal tides (Nash et al., 2012; Xu et al., 2013; Cao et al., 2017).

Acknowledgements

We thank UHSLC for providing water elevation records at the two tidal gauges used in this study.

References

Amin M. 1985. Temporal variations of tides on the west coast of Great Britain. Geophysical Journal International, 82(2): 279–299, doi: 10.1111/j.1365-246X.1985.tb05138.x

Caldwell P C, Merrifield M A, Thompson P R. 2015. Sea level measured by tide gauges from global oceans — the Joint Archive for Sea Level holdings (NCEI Accession 0019568), Version 5.5. NOAA National Centers for Environmental Information, Dataset, doi: 10.7289/V5V40S7W

Cao Anzhou, Guo Zheng, Lv Xianqing, et al. 2017. Coherent and incoherent features, seasonal behaviors and spatial variations of internal tides in the northern South China Sea. Journal of Marine Systems, 172: 75–83, doi: 10.1016/j.jmarsys.2017.03.005

Cherniawsky J Y, Foreman M G G, Kang S K, et al. 2009. 18.6-year lunar nodal tides from altimeter data. Continental Shelf Research, 30(6): 575–587

Codiga D L. 2011. Unified tidal analysis and prediction using the UTide matlab functions. Technical Report 2011–01. Narragansett, RI: Graduate School of Oceanography, University of Rhode Island

Devlin A T, Zaron E D, Jay D A, et al. 2018. Seasonality of tides in southeast Asian waters. Journal of Physical Oceanography, 48(5): 1169–1190, doi: 10.1175/JPO-D-17-0119.1

Doodson A T. 1921. The harmonic development of the tide-generating potential. Proceedings of the Royal Society A: Mathematical, Physical and Engineering Sciences, 100(704): 305–329

Doodson A T. 1924. Perturbations of harmonic tidal constants. Proceedings of the Royal Society of A: Mathematical, Physical and Engineering Sciences, 106(739): 513–526

Doodson A T. 1928. VI. The analysis of tidal observations. Philosophical Transactions of the Royal Society A: Mathematical. Physical and Engineering Sciences, 227(647–658): 223–279

Dunphy M, Lamb K G. 2014. Focusing and vertical mode scattering of the first mode internal tide by mesoscale eddy interaction. Journal of Geophysical Research: Oceans, 119(1): 523–536, doi: 10.1002/2013JC009293

Fang Guohong, Wang Yonggang, Wei Zexun, et al. 2004. Empirical cotidal charts of the Bohai, Yellow, and East China Seas from 10 years of TOPEX/Poseidon altimetry. Journal of Geophysical Research: Oceans, 109(C11): C11006, doi: 10.1029/2004JC002484

Feng Xiangbo, Tsimplis M N, Woodworth P L. 2015. Nodal variations and long-term changes in the main tides on the coasts of China. Journal of Geophysical Research: Oceans, 120(2): 1215–1232, doi: 10.1002/2014JC010312

Foreman M G G. 1977. Manual for tidal heights analysis and prediction. Patricia Bay: Institute of Ocean Sciences

Foreman M G G, Henry R F. 1989. The harmonic analysis of tidal model time series. Advances in Water Resources, 12(3): 109–120

Georgas N. 2012. Large seasonal modulation of tides due to ice cover friction in a midlatitude estuary. Journal of Physical Oceanography, 42(3): 352–369, doi: 10.1175/JPO-D-11-063.1

Godin G. 1972. The Analysis of Tides. Toronto, Canada: University of Toronto Press

Goldsbrough G R. 1942. Admiralty Manual of Tides. Nature, 150: 615–617, doi: 10.1038/150615a0

Gräwe U, Burchard H, Müller M, et al. 2014. Seasonal variability in M2 and M4 tidal constituents and its implications for the coastal residual sediment transport. Geophysical Research Letters, 41(15): 5563–5570, doi: 10.1002/2014GL060517

Guo Zheng, Pan Haidong, Cao Anzhou, et al. 2018. A harmonic analysis method adapted to capturing slow variations of tidal amplitudes and phases. Continental Shelf Research, 164: 37–44, doi: 10.1016/j.csr.2018.06.005

Huess V, Andersen O B. 2001. Seasonal variation in the main tidal constituent from altimetry. Geophysical Research Letters, 28(4): 567–570, doi: 10.1029/2000GL011921

Jay D A. 2009. Evolution of tidal amplitudes in the eastern Pacific Ocean. Geophysical Research Letters, 36(4): L04603

Jin Guangzhen, Pan Haidong, Zhang Qilin, et al. 2018. Determination of harmonic parameters with temporal variations: An enhanced harmonic analysis algorithm and application to internal tidal currents in the South China Sea. Journal of Atmospheric and Oceanic Technology, 35(7): 1375–1398, doi: 10.1175/JTECH-D-16-0239.1

Kang S K, Foreman M G, Lie H J, et al. 2002. Two - layer tidal modeling of the Yellow and East China Seas with application to seasonal variability of the M2 tide. Journal of Geophysical Research: Oceans, 107(C3): 6-1–6-18

Müller M. 2011. Rapid change in semi-diurnal tides in the North Atlantic since 1980. Geophysical Research Letters, 38(11): L11602

Müller M, Cherniawsky J Y, Foreman M G G, et al. 2014. Seasonal variation of the M2 tide. Ocean Dynamics, 64(2): 159–177, doi: 10.1007/s10236-013-0679-0

Nash J D, Shroyer E L, Kelly S M, et al. 2012. Are any coastal internal tides predictable?. Oceanography, 25(2): 80–95, doi: 10.5670/oceanog.2012.44

Pawlowicz R, Beardsley B, Lentz S. 2002. Classical tidal harmonic analysis including error estimates in MATLAB using T_TIDE.

Computers & Geosciences, 28(8): 929–937
Ray R D. 2006. Secular changes of the M_2 tide in the Gulf of Maine. Continental Shelf Research, 26(3): 422–427
Ray R D. 2009. Secular changes in the solar semidiurnal tide of the western North Atlantic Ocean. Geophysical Research Letters, 36(19): L19601, doi: 10.1029/2009GL040217
Stewart R H. 2008. Introduction to Physical Oceanography. College Station: Texas A&M University
St-Laurent P, Saucier F J, Dumais J F. 2008. On the modification of tides in a seasonally ice-covered sea. Journal of Geophysical Research: Oceans, 113(C11): C11014
Woodworth P L. 2010. A survey of recent changes in the main components of the ocean tide. Continental Shelf Research, 30(15): 1680–1691, doi: 10.1016/j.csr.2010.07.002
Xu Zhenhua, Yin Baoshu, Hou Yijun, et al. 2013. Variability of internal tides and near-inertial waves on the continental slope of the northwestern South China Sea. Journal of Geophysical Research: Oceans, 118(1): 197–211, doi: 10.1029/2012JC008212

Appendix:

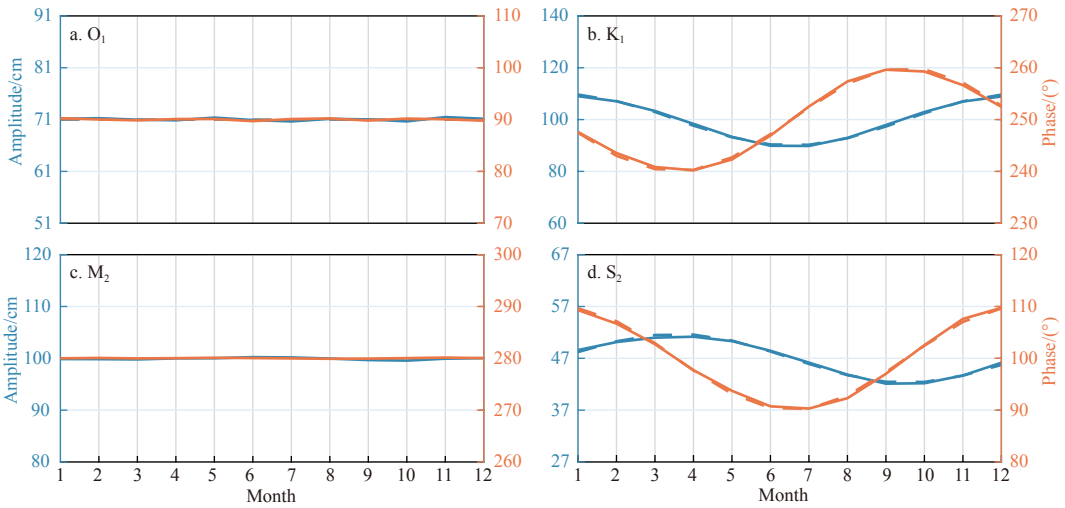

Fig. A1. Monthly amplitudes (blue solid lines) and phase lags (orange solid lines) of the O_1 (a), K_1 (b), M_2 (c) and S_2 (d) constituents for the two-step HA in IE 2. The dashed lines in b and d denote the prescribed amplitudes and phase lags at the center of each month.

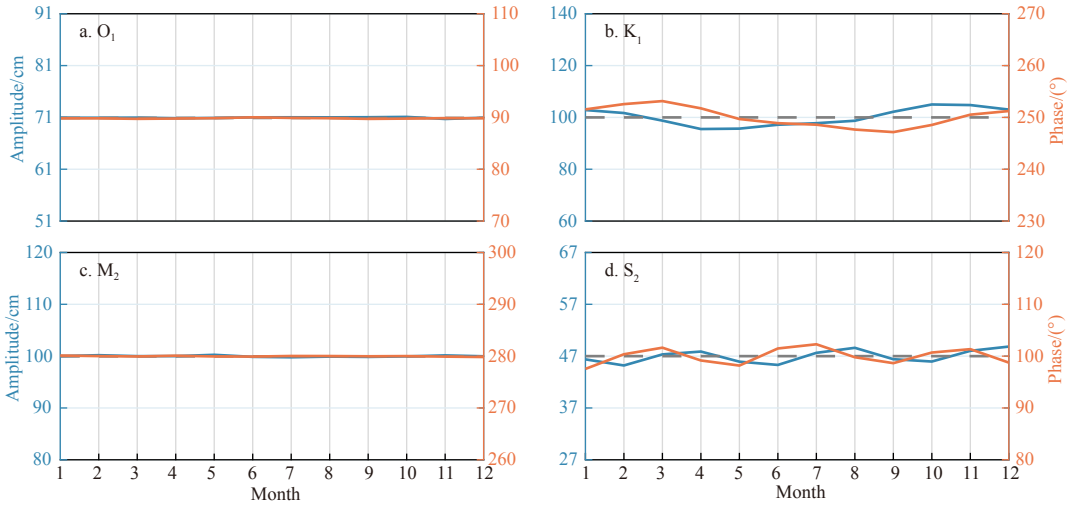

Fig. A2. Monthly amplitudes (blue solid lines) and phase lags (orange solid lines) of the O_1 (a), K_1 (b), M_2 (c) and S_2 (d) constituents for the two-step HA in IE 3. The dashed lines in b and d denote the prescribed amplitudes and phase lags at the center of each month.

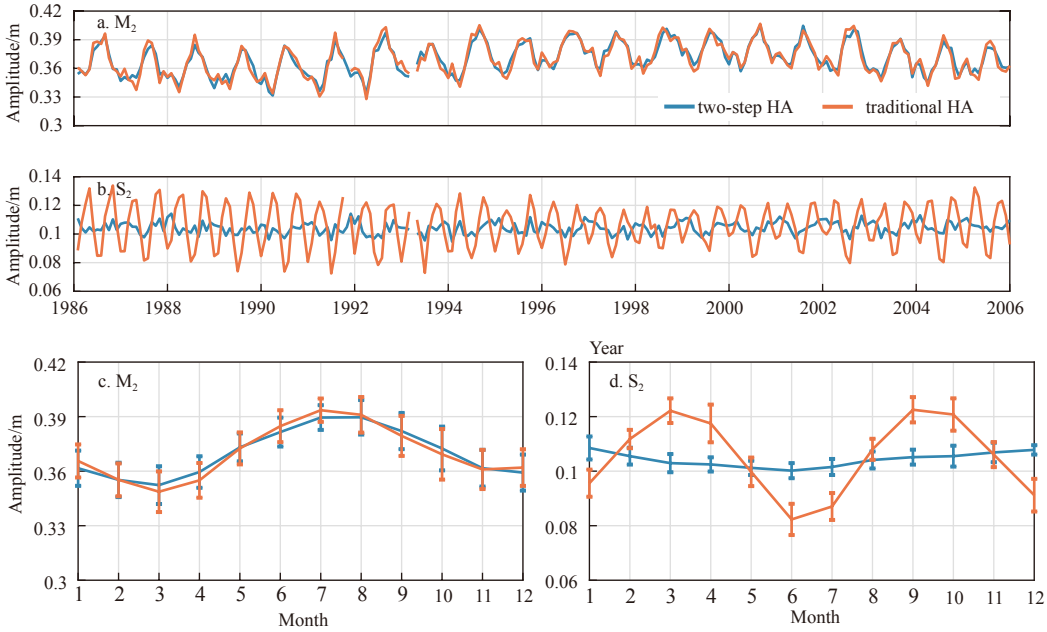

Fig. A3. Monthly amplitudes of the M_2 (a) and S_2 (b) constituents at Victoria during 1966–1985, and the 20-year-averaged monthly amplitudes and corresponding STDs of the M_2 (c) and S_2 (d) constituents. In each subfigure, the blue and orange lines denote the results obtained by the two-step HA and traditional HA using a one-month window, respectively.

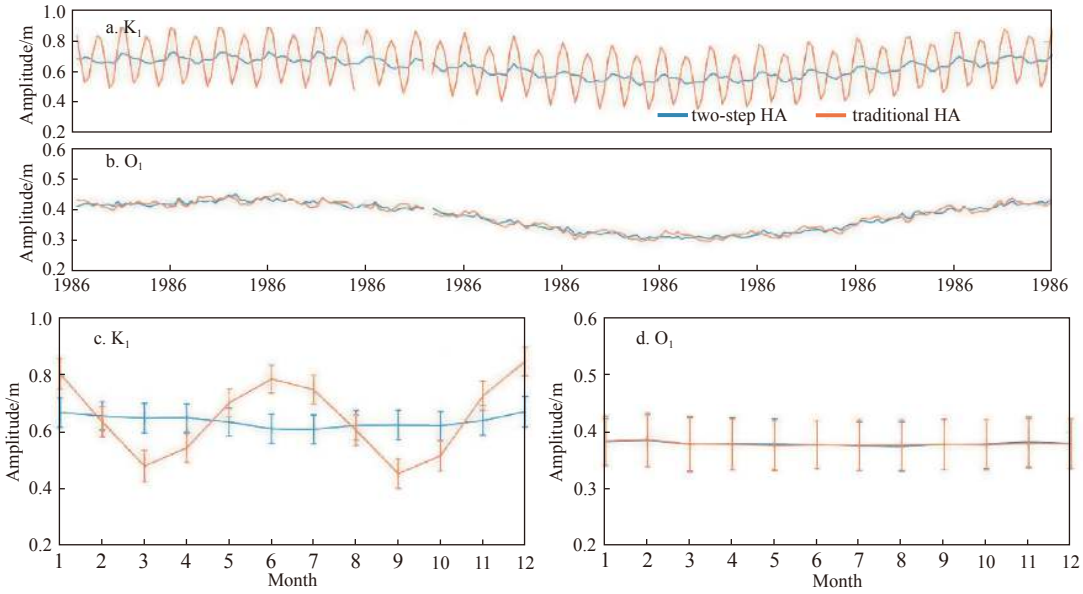

Fig. A4. Monthly amplitudes of the K_1 (a) and O_1 (b) constituents at Victoria during 1966–1985， and the 20-year-averaged monthly amplitudes and corresponding STDs of the K_1 (c) and O_1 (d) constituents. In each subfigure, the blue and orange lines denote the results obtained by the two-step HA and traditional HA using a one-month window, respectively.